

Kinetic studies on axial coordination reactions of *para*-substituted tetraphenylporphinatoiron(III) chlorides

Yun-Ti Chen*, Zhiang Zhu and Yuxin Ma

Department of Chemistry, Nankai University, Tianjin 300071 (China)

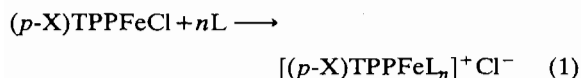
(Received February 6, 1990; revised June 15, 1990)

Abstract

A series of *para*-substituted tetraphenylporphinatoiron(III) chlorides [(*p*-X)TPPFeCl] (X = Cl, H, CH₃, OCH₃) have been synthesized. Kinetic studies are reported for the reactions of (*p*-X)TPPFeCl + *n*L → [(*p*-X)TPPFeL_{*n*}] + Cl⁻ (L = imidazole, 2-methylimidazole and 2-ethyl-4-methyl-imidazole) in acetone at several temperatures. The reaction rates are second order dependent on Im and MeIm with *n* = 2, but first order on EMIm with *n* = 1; the reaction rates increase with temperature in both cases. The mechanisms of reactions for various ligands have been proposed. The effects of various ligands and *para*-substituents on the phenyl rings for these reactions have been investigated.

Introduction

Variations in the biological role of the naturally occurring heme proteins are intimately associated with changes in the axial ligation and substituent of the heme moiety [1]. Relevant to our understanding of the mechanism of the action of the heme proteins is an understanding of the manner in which axial ligation and substituent affect the electronic structure and reactivity of a metalloporphyrin system. The physical properties (electronic [2], NMR [3], ESR [4], Mössbauer spectra [5]), thermodynamic [6] and kinetic [7] aspects have been studied by many investigators. Because of its structural features, the series of *ms*-tetraphenylporphinatoiron complexes are a good model system for the study of substituent effect. Sweigart and coworkers [8] initially reported the reaction of ferric porphyrin with imidazole at 25 °C and discussed the effect of the hydrogen bond on the reaction dynamics. In this paper we report the kinetic studies on a series of *para*-substituted tetraphenylporphinatoiron(III) chloride complexes reacting with three axial ligands L (L = imidazole(Im), 2-methylimidazole(MeIm), 2-ethyl-4-methylimidazole(EMIm)) in acetone at several temperatures.



We have previously determined *n* = 2 for Im and MeIm but *n* = 1 for EMIm [9]. The steric and electronic effects of the axial ligands on mechanisms and rate constants have been compared and the substituent effect has been discussed. It has been found that an isokinetic relationship and linear free energy relationship exist in the system studied.

Experimental

Materials

All reactions and distillations were carried out in rigorously water-free glassware. All solvents and EMIm were of analytical reagent grades and acetone was further purified according to the standard procedure [10]. Im and MeIm were recrystallized twice from absolute alcohol and dried *in vacuo*. The series of (*p*-X)TPP and (*p*-X)TPPFeCl were prepared and purified using literature methods [11, 12] and were characterized by comparison with published UV-Vis absorption spectra [13].

Measurements

Kinetic measurements were carried out in acetone under pseudo-first order conditions with the ligands concentrations in at least 100-fold excess over that of (*p*-X)TPPFeCl. The measurements were made by means of a Union Giken RA-401 stopped-flow instrument and a Shimadzu UV-240 spectrophotometer in the temperature range 5–35 (±0.1) °C and

*Author to whom correspondence should be addressed.

at $\lambda=510$ nm, where a decrease in absorbance of reactant occurred and the ligands showed no absorbance at this wavelength.

Results and discussion

For the pseudo-first order reactions, the observed rate constant k_{obs} of eqn. (1) was determined by the Guggenheim method [14].

Reactions of $(p\text{-X})\text{TPPF}e\text{Cl}$ with Im and MeIm

The series of $(p\text{-X})\text{TPPF}e\text{Cl}$ react rapidly with Im in acetone to give $[(p\text{-X})\text{TPPF}e(\text{Im})_2]^+\text{Cl}^-$, which have been measured by the stopped-flow method using a Union Giken RA-401 instrument in the temperature range 5–35 °C. Standard plots of $\ln(A-A_\infty)$ versus time were linear over 3–4 half-lives. The dependence of k_{obs} on Im concentration (C_L) is shown in Fig. 1. It has been found that plots of C_L/k_{obs} versus $1/C_L$ gave good linear relationships as shown in Fig. 2. These linear relationships may be expressed by eqn. (2).

$$C_L/k_{\text{obs}} = a + b/C_L \quad (2)$$

where a and b are constants. Rearrangement of eqn. (2) gives eqn. (3)

$$k_{\text{obs}} = \frac{(1/b)(a/b)C_L^2}{1 + (a/b)C_L} \quad (3)$$

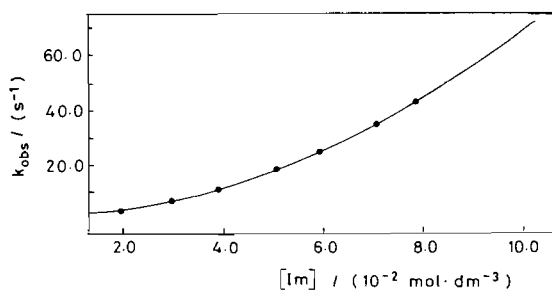


Fig. 1. Plot of k_{obs} vs. $[\text{Im}]$ at 25 °C, $\text{X}=\text{Cl}$.

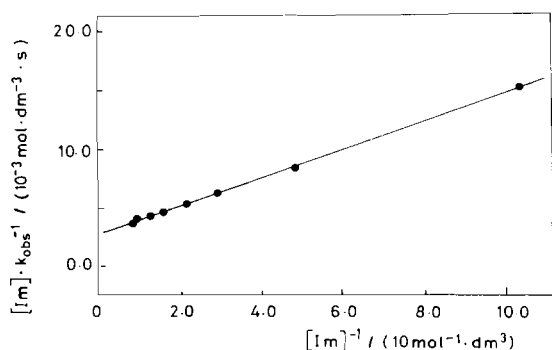
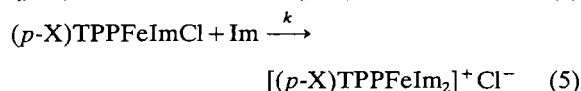
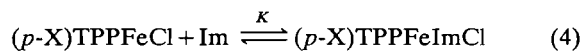


Fig. 2. Plot of $[\text{Im}]/k_{\text{obs}}$ vs. $1/[\text{Im}]$ at 25 °C, $\text{X}=\text{Cl}$.

It is well known that $K C_L/(1 + K C_L)$ is the distribution coefficient of the product in the equilibrium $\text{X} + \text{L} \rightarrow \text{XL}$. The proposed mechanism of reaction (1) ($\text{L}=\text{Im}$) is therefore considered reasonable in view of the above analysis as the following.



The first step (4) is a pre-equilibrium to form the six-coordinated intermediate. The second step (5) is a rate-determining-step (r.d.s) to form the product. From the above proposed mechanism the following rate equation may be derived.

$$-d[\text{P}]/dt = [k K C_L^2 / (1 + K C_L)] [\text{P}] \quad (6)$$

where P represents $(p\text{-X})\text{TPPF}e\text{Cl}$. Thus

$$k_{\text{obs}} = k K C_L^2 / (1 + K C_L) \quad (7)$$

Equation (7) is practically identical with eqn. (3) which was obtained from experiments by changing k to $1/b$ and K to a/b . It shows that k_{obs} should be proportional to C_L^2 when C_L is very small, which has been verified by the fact that the correlation coefficient of k_{obs} versus C_L^2 of the first four points in Fig. 1 is 0.999. It further supports the proposed mechanism.

According to eqn. (7), a least-squares minimization routine was compiled by means of the Gauss-Newton-Marquardt method [15] and the experimental data were fitted satisfactorily with the parameters K and k , whose values are shown in Tables 1 and 2, respectively. Changes of standard molar enthalpy ΔH_m° and molar entropy ΔS_m° in the pre-equilibrium step (4) as well as activation enthalpies $\Delta^\ddagger H_m$, activation entropies $\Delta^\ddagger S_m$ of the rate-determining step (5) were calculated and are also listed in Tables 1 and 2.

$(p\text{-Cl})\text{TPPF}e\text{Cl}$ reacts slowly with MeIm in acetone to give $[(p\text{-Cl})\text{TPPF}e(\text{MeIm})_2]^+\text{Cl}^-$ at 30 °C as compared with Im , which was measured using a Shimadzu UV-240 spectrophotometer by means of the spectral method. Since the experimental results are similar to that of Im , it implies that the mechanism of this reaction is essentially the same as proposed in eqns. (4) and (5). The experimental data were fitted satisfactorily with the parameters $K = 20.4(\pm 0.4) \text{ mol}^{-1} \text{ dm}^3$ and $k = 9.5(\pm 0.2) \times 10^3 \text{ s}^{-1}$.

Reaction of $(p\text{-Cl})\text{TPPF}e\text{Cl}$ with EMIm

$(p\text{-Cl})\text{TPPF}e\text{Cl}$ reacts with EMIm in acetone to give $[(p\text{-Cl})\text{TPPF}e(\text{EMIm})]^+\text{Cl}^-$, which were measured using a Shimadzu UV-240 spectrophotometer

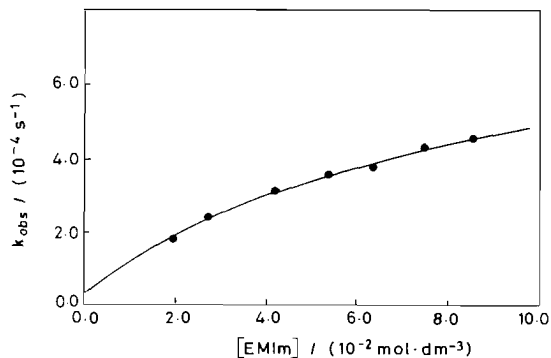
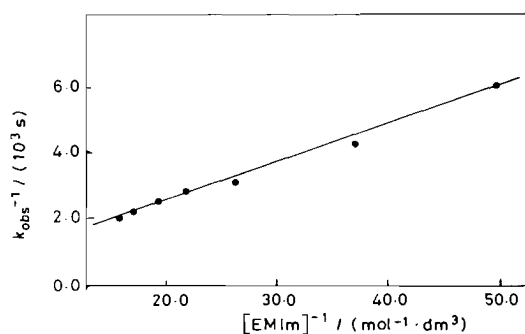
TABLE 1. Equilibrium constants, changes of standard molar enthalpy and molar entropy of eqn. (4) at different temperatures

	K (mol ⁻¹ dm ³)						ΔH_m^*	ΔS_m^*
	5 °C	15 °C	20 °C	25 °C	30 °C	35 °C	(kJ mol ⁻¹)	(J mol ⁻¹ K ⁻¹)
Cl		0.964	0.786	0.656	0.484	0.331	-38.6	-134
H		0.459	0.310	0.244	0.176	0.128	-46.1	-166
CH ₃		0.236	0.257	0.134	0.0984	0.0599	-64.1	-231
OCH ₃	0.668	0.166		0.0661		0.0275	-75.0	-274

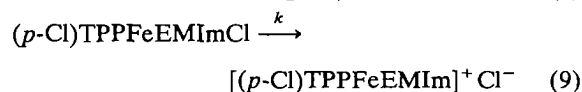
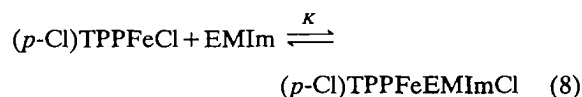
TABLE 2. Rate constants, activation enthalpies and entropies of eqn. (5) at different temperatures

	k (10 ³ s ⁻¹)						Δ^*H_m	Δ^*S_m
	5 °C	15 °C	20 °C	25 °C	30 °C	35 °C	(kJ mol ⁻¹)	(J mol ⁻¹ K ⁻¹)
Cl		5.48	7.76	10.9	16.5	25.1	53.6	12.6
H		9.58	16.1	21.6	33.5	49.6	57.2	30.3
CH ₃		13.0	18.0	36.8	56.6	99.6	74.6	92.3
OCH ₃	6.12	28.5		85.0		253	85.1	134

in the temperature range 25–40(±0.1) °C. If this reaction proceeded in one step, the pseudo-first order rate constant would be directly proportional to EMIm concentrations. However, this did not happen (see Fig. 3), while the plots of $1/k_{\text{obs}}$ versus $1/[\text{EMIm}]$ gave good linear relationships as shown in Fig. 4. Therefore, the mechanism of the reaction should be

Fig. 3. Plot of k_{obs} vs. $[\text{EMIm}]$ at 25 °C, X=Cl.Fig. 4. Plot of $1/k_{\text{obs}}$ vs. $1/[\text{EMIm}]$ at 25 °C, X=Cl.

different from that of Im and is shown by eqns. (8) and (9). The reaction rate constant may be expressed by eqn. (10).



$$k_{\text{obs}} = kK[\text{EMIm}]/(1 + K[\text{EMIm}]) \quad (10)$$

According to eqn. (10), experimental data were fitted satisfactorily with the parameters K and k whose values are given in Table 3; ΔH_m^* , ΔS_m^* of the pre-equilibrium step and Δ^*H_m , Δ^*S_m of the rate-determining step are also listed in Table 3.

Effect of axial ligands

The three ligands employed for the axial coordination reaction have different numbers n (for Im and MeIm $n=2$, for EMIm $n=1$) and proceed with different mechanisms as mentioned above, because of the difference of their electronic effect and steric effect. The kinetic parameters obtained from the experiments are listed in Tables 1, 2 and 3, respectively. It shows that the pre-equilibrium steps for all ligands are an exothermic process with entropy degradation.

The stability of the six-coordination intermediate is dependent not only on the steric inhibition of the attack direction, but also on the nucleophilic ability of the ligand. The order of the steric inhibition of the ligands as well as the nucleophilic ability is

TABLE 3. Parameters of reaction of EMIm with (*p*-Cl)TPPFeCl at different temperatures

	25 °C	30 °C	35 °C	40 °C
K (mol ⁻¹ dm ³)	11.9	11.8	10.9	9.57
k (10 ⁻³ s ⁻¹)	0.85	0.92	1.19	1.22
ΔH_m° (kJ mol ⁻¹)	-11.2			
Δ^*H_m (kJ mol ⁻¹)	18.6			
ΔS_m° (J mol ⁻¹ K ⁻¹)	-16.8			
Δ^*S_m (J mol ⁻¹ K ⁻¹)	-43.7			

EMIm > MeIm > Im. However these two effects operate conversely and the order of the pre-equilibrium constants is as follows $K(\text{MeIm}) > K(\text{EMIm}) > K(\text{Im})$. $K(\text{Im})$ is the lowest due to its low nucleophilic ability. Although the nucleophilic ability of EMIm is a bit larger than MeIm, the ligand EMIm has a larger steric inhibition which diminishes its K value.

As the ligand combines with the central iron ion to form the Fe–N bond with an accompanying liberation of energy, ΔH_m° of the pre-equilibrium step has a negative value. The strength of the Fe–N bond depends not only on the energies of the metal d_π orbital and ligand π orbital, but also on steric effect. Since the ligand EMIm exhibits a larger steric effect than Im, the strength of its Fe–N bond might be weaker and liberate less energy, thus $|\Delta H_m^\circ(\text{EMIm})| < |\Delta H_m^\circ(\text{Im})|$. The pre-equilibrium step is a process of diminishing species, ΔS_m° has therefore a negative value. The ligands in acetone are associated through hydrogen bonding [16] and the association of EMIm is easier than Im. Therefore the translation degree of freedom is less for EMIm. The entropy decrease of the pre-equilibrium step of EMIm is smaller than that of Im.

The order of rate constants is $k(\text{EMIm}) < k(\text{MeIm}) < k(\text{Im})$. This order may be interpreted by the steric inhibition effect. Appreciable van der Waals repulsions probably occur between the π system of the iron–porphyrin and methyl group or ethyl group of EMIm. The order of steric effect of the ligands is EMIm > MeIm > Im. The steric inhibition of EMIm is so large that even the second bulky EMIm molecule cannot approach the central iron ion.

The r.d.s. for the ligand Im was that Cl on the six-coordinated Fe(III) was substituted by the nucleophilic ligand Im. The ligand field theory [17] states that when a substitution reaction takes place in a six-coordinated complex with a central metal ion having more than three d-electrons, the dissociation mechanism would be favorable with respect to the association mechanism. Furthermore, the dissociated group of the rate-determining step would

be Cl which could form a H bond with the ligand in solution and would promote dissociation from (*p*-X)TPPFeImCl, so in r.d.s., Cl dissociates first, followed by the second ligand Im attack to form the product. Since dissociation of Cl requires energy, the activation enthalpy is positive.

For the dissociative mechanism the activation entropy Δ^*S_m should have a positive value, however the contribution of a large negative solvation entropy would offset Δ^*S_m to some extent. For the reaction of EMIm the contribution of solvation entropy is predominant, and its Δ^*S_m value is negative.

Effect of *para*-substituents on the phenyl rings

The effect of *para*-substituent groups on the phenyl rings upon the pre-equilibrium step (4) may be seen from the data shown in Table 1. The orders of K , ΔH_m° , ΔS_m° of the pre-equilibrium step are as follows $K(\text{Cl}) > K(\text{H}) > K(\text{CH}_3) > K(\text{OCH}_3)$, $|\Delta H_m^\circ(\text{Cl})| < |\Delta H_m^\circ(\text{H})| < |\Delta H_m^\circ(\text{CH}_3)| < |\Delta H_m^\circ(\text{OCH}_3)|$, $|\Delta S_m^\circ(\text{Cl})| < |\Delta S_m^\circ(\text{H})| < |\Delta S_m^\circ(\text{CH}_3)| < |\Delta S_m^\circ(\text{OCH}_3)|$. These orders may be interpreted in accordance with the fact that the electron-donating substituent increases the electron density on the pyrrole-nitrogen atoms of the porphyrin, which is not favorable for the nucleophilic axial ligand to attack the central ion and thus decreases the pre-equilibrium constant K . According to the ligand field theory [16] the enhancement of electron density would increase the splitting energy Dq of the ligand field which increases $|\Delta H_m^\circ|$ of the pre-equilibrium step. Thus the stronger the electron-donating ability of the substituents, the larger is the $|\Delta H_m^\circ|$ value of the pre-equilibrium step.

Table 2 shows the effect of *para*-substituents on the rate-determining step. The orders of magnitude of rate constants for different substituents are as follows: $k(\text{Cl}) < k(\text{H}) < k(\text{CH}_3) < k(\text{OCH}_3)$, $\Delta^*H_m(\text{Cl}) < \Delta^*H_m(\text{H}) < \Delta^*H_m(\text{CH}_3) < \Delta^*H_m(\text{OCH}_3)$, $\Delta^*S_m(\text{Cl}) < \Delta^*S_m(\text{H}) < \Delta^*S_m(\text{CH}_3) < \Delta^*S_m(\text{OCH}_3)$. It shows that the stronger the electron-donating ability of the substituent, the larger are the rate-determining constant k and Δ^*H_m and Δ^*S_m values. The rate-

determining step (7) is an axial ligand exchange reaction and proceeds according to a dissociative mechanism. The electron-donating substituent increases the electron density of the pyrrole-nitrogen atoms of the porphyrin and the splitting energy of the ligand field Dq value as well. The increment of the electron density favours the dissociation of Cl from (*p*-X)TPPFeImCl, therefore the rate increases with the ability of electron-donation. The more the Cl dissociates, the larger is the degree of disorder, which is reflected by the Δ^*S_m value. The activation enthalpy Δ^*H_m increases as a result of the increase of Dq .

LFER and isokinetic relationships

It was found that several linear free energy relationships exist between the kinetic and thermodynamic parameters and the Hammett σ constant in the system studied and they are listed as follows.

15 °C, $\ln K = 0.82(4\sigma) - 0.76$, $r = 0.992$; $\ln k = -0.75(4\sigma) + 9.2$, $r = 0.95$;

25 °C, $\ln K = 1.10(4\sigma) - 1.41$, $r = 0.992$; $\ln k = -0.96(4\sigma) + 10.1$, $r = 0.97$;

35 °C, $\ln K = 1.20(4\sigma) - 2.14$, $r = 0.992$; $\ln k = -1.09(4\sigma) + 11.0$, $r = 0.97$;

$\Delta H_m^\ddagger = 18.3(4\sigma) - 52.1$, $r = 0.96$; $\Delta S_m^\ddagger = 70.0(4\sigma) - 1.86 \times 10^2$, $r = 0.97$;

$\Delta^*H_m = -15.9(4\sigma) + 64.3$, $r = 0.94$; $\Delta^*S_m = -60.9(4\sigma) + 54.7$, $r = 0.95$.

It is interesting to note that some isokinetic relationship, which was first labelled by Leffler [18] and then called the compensation law by Brown [19], has also been found to exist between ΔH and ΔS of the system studied as follows

$$\Delta^*H_m = 262.7, \Delta^*S_m + 49.89, \quad r = 0.999$$

and the isokinetic temperature β was found to be 262.7 K.

References

- 1 J. I. Aihara, M. Tsuda and H. Inokuchi, *Bull. Chem. Soc. Jpn.*, **42** (1969) 1824.
- 2 M. Meot-Ner and A. D. Adler, *J. Am. Chem. Soc.*, **97** (1975) 5107.
- 3 D. Dolphin, *The Porphyrins*, Vol. IV, Academic Press, London, 1979.
- 4 W. R. Scheidt and C. A. Reed, *Chem. Rev.*, **81** (1981) 543.
- 5 (a) B. Lukas and J. Silver, *Inorg. Chim. Acta*, **124** (1986) 97; (b) J. Silver and B. Lukas, *Inorg. Chim. Acta*, **126** (1987) 99.
- 6 V. L. Balke, F. A. Walker and J. T. West, *J. Am. Chem. Soc.*, **107** (1985) 1226.
- 7 (a) G. A. Tondreau and D. A. Sweigart, *Inorg. Chem.*, **23** (1984) 1060. (b) J. G. Jones, G. A. Tondreau, J. O. Edwards and D. A. Sweigart, *Inorg. Chem.*, **24** (1985) 296.
- 8 A. Mahmood, H. L. Lin, J. G. Jones, J. O. Edwards and D. A. Sweigart, *Inorg. Chem.*, **27** (1988) 2149.
- 9 Y. X. Ma, Z. A. Zhu and Y. T. Chen, *Thermochem. Acta*, (1990) in press.
- 10 D. D. Perrin, W. L. F. Armarego and D. R. Perrin, *Purification of Laboratory Chemicals*, Pergamon, Oxford, 1980.
- 11 A. D. Adler, *J. Org. Chem.*, **32** (1967) 476.
- 12 A. D. Adler and F. R. Longo, *J. Inorg. Nucl. Chem.*, **32** (1970) 2443.
- 13 H. Kobayashi, T. Higuchi, Y. Kaizu, H. Osada and M. Aoki, *Bull. Chem. Soc. Jpn.*, **48** (1975) 3137.
- 14 J. W. Moore and R. G. Pearson, *Kinetics and Mechanism*, Wiley, New York, 3rd edn., 1981.
- 15 J. Q. Xue, *The Principle and Methods of Optimization*, Yejin Gongye Press, 1983 (in Chinese).
- 16 F. A. Walker, M. W. Lo and M. T. Ree, *J. Am. Chem. Soc.*, **98** (1976) 5552.
- 17 H. L. Schäfer and G. Gliemann, translated by D. F. Ilten, *Basic Principles of Ligand Field Theory*, Wiley, London, 1982.
- 18 J. E. Leffler, *J. Org. Chem.*, **20** (1955) 1202.
- 19 R. F. Brown, *J. Org. Chem.*, **27** (1962) 3015.